

Inhomogeneous Thermalization in Strongly Coupled Field Theories

V. Balasubramanian,^{1,2} A. Bernamonti,³ J. de Boer,⁴ B. Craps,⁵ L. Franti,⁶ F. Galli,⁵ E. Keski-Vakkuri,^{6,7}
B. Müller,^{8,9} and A. Schäfer¹⁰

¹*David Rittenhouse Laboratory, University of Pennsylvania, Philadelphia, Pennsylvania 19104, USA*

²*Laboratoire de Physique Théorique, École Normale Supérieure, 75005 Paris, France*

³*Instituut voor Theoretische Fysica, KU Leuven, Celestijnenlaan 200D, B-3001 Leuven, Belgium*

⁴*Institute for Theoretical Physics, University of Amsterdam, 1090 GL Amsterdam, The Netherlands*

⁵*Theoretische Natuurkunde, Vrije Universiteit Brussel, and International Solvay Institutes, B-1050 Brussels, Belgium*

⁶*Helsinki Institute of Physics & Department of Physics, FIN-00014 University of Helsinki, Finland*

⁷*Department of Physics and Astronomy, Uppsala University, SE-75108 Uppsala, Sweden*

⁸*Department of Physics, Duke University, Durham, North Carolina 27708, USA*

⁹*Brookhaven National Laboratory, Upton, New York 11973, USA*

¹⁰*Institut für Theoretische Physik, Universität Regensburg, D-93040 Regensburg, Germany*

(Received 29 July 2013; published 4 December 2013)

To describe theoretically the creation and evolution of the quark-gluon plasma, one typically employs three ingredients: a model for the initial state, nonhydrodynamic early time evolution, and hydrodynamics. In this Letter we study the nonhydrodynamic early time evolution using the AdS/CFT correspondence in the presence of inhomogeneities. We find that the AdS description of the early time evolution is well matched by free streaming. Near the end of the early time interval where our analytic computations are reliable, the stress tensor agrees with the second order hydrodynamic stress tensor computed from the local energy density and fluid velocity. Our techniques may also be useful for the study of far-from-equilibrium strongly coupled systems in other areas of physics.

DOI: [10.1103/PhysRevLett.111.231602](https://doi.org/10.1103/PhysRevLett.111.231602)

PACS numbers: 11.25.Tq, 52.27.Gr

Strongly coupled quantum liquids are studied in many settings: (a) quark-gluon matter in ultrarelativistic heavy ion collisions, (b) strongly correlated electrons in metals, cuprates, and heavy-fermion materials, and (c) condensates of ultracold atoms. The holographic gauge-gravity framework provides insights into the dynamics of such fluids. Specifically, the fluid-gravity correspondence [1] permits derivation of complete second order hydrodynamic equations for conformal relativistic fluids from Einstein's equations in a long wavelength limit [2,3]. Here we use an analytically tractable model to further ask how a far-from-equilibrium, inhomogeneous initial state approaches a regime well-approximated by hydrodynamics.

RHIC and LHC experiments show that at times even earlier than 1 fm/c, matter produced in heavy ion collisions exhibits hydrodynamic collective behavior. Notably, one observes “elliptic flow”—a $\cos(2\phi)$ correlation between the azimuthal momentum direction of produced hadrons and the collision plane [4–7]. This is also deduced from azimuthal two-particle correlations among emitted hadrons (the “ridge” or “double-ridge” effect in Pb + Pb collisions at the LHC [7–10]).

Experimentally, odd and even Fourier flow coefficients for central heavy ion collisions are similar [7,8,11]. By symmetry, odd coefficients can only be generated by fluctuations [12,13], so fluctuations are large. The parton saturation model for the nuclear state suggests initial fluctuations in the plane transverse to the beam are short range (of order of the inverse saturation scale $1/Q_s \sim 0.2$ fm [14]).

Simulations [15–17] use models (e.g., the Color Glass Condensate) to evolve the initial energy deposits briefly ($t \leq 0.4$ fm/c) using classical Yang-Mills equations. These studies fit all flow coefficients by assuming that large-amplitude, small-range fluctuations subsequently evolve hydrodynamically. For times short compared to the scale of the background Yang-Mills field, (~ 0.2 fm/c), classical Yang-Mills theory is kinetic energy dominated and should be well-approximated by a free-streaming model. Alternate approaches start from nucleon position fluctuations and energy deposition in individual nucleon collisions [18,19] and use free-streaming of particles [20] or hydrodynamics of anisotropic fluids [21,22] to bridge the gap to the onset of viscous hydrodynamics. There is a key open question: to what extent can this “gluing” of a phenomenological model describing the initial evolution to viscous hydrodynamics be justified?

Thermalization in strongly coupled conformal field theories with a gravity dual corresponds to black brane formation in asymptotically anti-de Sitter (AdS) spacetimes [23]. In general, this requires a numerical approach, but analytical calculations are sometimes possible. In the context of a massless scalar field minimally coupled to gravity in $d + 1$ space-time dimensions with negative cosmological constant, [24] considered the effect of homogeneous boundary sources. They turned on a brief ($0 < t < \delta t$) source $\phi_0(t) = \epsilon \tilde{\phi}_0(t)$ for a marginal operator corresponding to the massless scalar field in the bulk and solved the field equations perturbatively in ϵ . In $d + 1$ bulk

dimensions and to second order in ϵ , they found the AdS-Vaidya metric

$$ds^2 = -\left(r^2 - \frac{M(v)}{r^{d-2}}\right)dv^2 + 2dvdr + r^2 d\vec{x}^2 + \mathcal{O}(\epsilon^4), \quad (1)$$

where $M(v)$ vanishes for $v < 0$ and is otherwise of order $\epsilon^2/(\delta t)^d$ (we have set $R_{\text{AdS}} = 1$). For odd d , M is constant for $v > \delta t$ and the geometry describes a black brane with temperature $\sim \epsilon^{2/d}/\delta t$. This space-time describes a shell of null dust falling in from the AdS boundary to form a black brane. At the boundary, the Eddington-Finkelstein coordinate v coincides with the field theory time t . Figure 1 shows a schematic representation. The weak-field approximation considers injection times short compared to the inverse temperature of the black brane to be formed.

Naive perturbation theory in ϵ is reliable for $v \ll 1/T$, but diverges for $v \gg 1/T$. A resummed perturbation theory can be defined by expanding around the AdS-Vaidya geometry (1) rather than AdS, i.e., by working exactly in $M(v)$ and perturbatively in all other occurrences of ϵ [24]. (This is analogous to absorbing temperature-dependent masses in propagators in thermal perturbation theory.) This approach is technically more complicated, but it was shown in [24] that resummed perturbation theory is reliable everywhere outside the event horizon. For late times ($v \gg 1/T$), observables decay exponentially to their thermal values, with relaxation times of order of the inverse temperature.

In the AdS-Vaidya model thermalization proceeds at the speed of light [25–28], at least for the range of length scales studied in [27,28]. (For $d > 2$, thermalization happens at a smaller speed on length scales larger than the inverse temperature [29].) However, the initial state of heavy ion collisions has strong asymmetries between longitudinal and transverse pressures (strong longitudinal gauge fields may even make the former negative initially), and large transverse density. The effect of the pressure anisotropy was studied assuming longitudinal boost invariance and transverse homogeneity in [30–32], where it was found that hydrodynamic behavior is reached on time

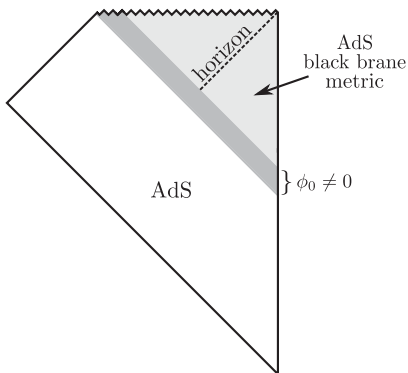


FIG. 1. A schematic representation of the dynamical collapse process first studied in [24].

scales $\sim 0.3\text{--}0.5$ fm/ c for many different initial conditions. This “hydroization” is not equivalent to complete thermalization because viscous hydrodynamic behavior at early times in a boost invariant expansion implies a large pressure anisotropy and thus strong deviation from local thermal equilibrium. Here, we instead analyze how the approach to hydrodynamic behavior is affected by local density fluctuations.

In a companion paper [33], we generalize the construction of [24] to an inhomogeneous scalar field source that turns on at some time. As in [24], we solve the equations of motion perturbatively in the amplitude of the scalar field boundary value, now allowed to depend on the spatial coordinates. For analytical control we make the simplifying assumption (suggested in [24]) that the scale of spatial variations is large compared with all other scales. (In a heavy ion context, this assumption is not justified for fluctuations at a scale $1/Q_s$, which is smaller than the inverse temperature, so some extrapolation will be needed to make contact with those.) As in [24], a four-dimensional bulk space-time is technically simpler than the five-dimensional one. Since in heavy ion collisions azimuthal anisotropies are studied in the directions transverse to the beam, a four-dimensional bulk geometry may not constitute a serious limitation. More realistic models would involve nearly boost invariant geometries or colliding inhomogeneous shock waves, but for computational tractability these will not be studied here. To simplify further, we consider the simplest case—an asymptotically AdS₄ geometry with inhomogeneities along one spatial direction.

Specifically, we construct the bulk solution for the scalar field and the metric up to second order in the amplitude of the source that drives the gravitational collapse and up to fourth order in the gradient expansion. For instance, up to second order in the amplitude of the source $\varphi(v, x)$ and up to fourth order in spatial gradients, solving the coupled equations of motion for the metric and scalar field ϕ gives

$$\phi = \varphi(v, x) + \frac{\dot{\varphi}(v, x)}{r} + \frac{\varphi''(v, x)}{2r^2} + \frac{\int_{-\infty}^v d\tau \varphi''''(\tau, x)}{8r^3} + \dots \quad (2)$$

Similar expressions can be obtained for other metric components. Our solutions are reliable for times v short compared to the inverse local temperature $T(x)$ (of the black brane to be formed) and local scales of variation $L(x)$ large compared to the inverse temperature, $v \ll 1/T(x) \ll L(x)$. From these solutions, we extract the expectation value of the boundary energy-momentum tensor, and study its time evolution after the inhomogeneous energy injection. Specifically, $\langle T_{\alpha\beta} \rangle \sim g_{(3)\alpha\beta}$, where $g_{(3)}$ is the $1/r$ coefficient of the bulk metric in Fefferman-Graham coordinates. For instance, up to second order in the amplitude expansion and in the derivative expansion,

$$\begin{aligned}
T_{tt}(t, x) = & -\frac{1}{16\pi G_N} \left\{ \frac{1}{2} \int_{-\infty}^t d\tau \left[2\dot{\varphi}(\tau, x)\ddot{\varphi}(\tau, x) \right. \right. \\
& - (\dot{\varphi}'(\tau, x))^2 - 4\dot{\varphi}(\tau, x)\dot{\varphi}''(\tau, x) \\
& + 2\ddot{\varphi}(\tau, x)\varphi''(\tau, x) + 2\ddot{\varphi}'(\tau, x)\varphi'(\tau, x) \\
& + 2\frac{\partial}{\partial x} \int_{-\infty}^{\tau} ds \left[\dot{\varphi}(s, x)\dot{\varphi}'(s, x) \right. \\
& \left. \left. - \int_{-\infty}^s dw \dot{\varphi}'(w, x)\dot{\varphi}(w, x) \right] \right\}. \quad (3)
\end{aligned}$$

To compute the evolution for later times, a resummation of perturbation theory would be required, but this is beyond the scope of the present work, in which we restrict ourselves to the early-time evolution. From the energy-momentum tensor, we compute the local velocity $V(t, x)$ (i.e., the velocity relative to the lab frame of the local rest frame in which the stress-tensor becomes diagonal), as well as the energy density $\varepsilon(t, x)$ and pressure components $p_x(t, x)$, $p_y(t, x)$ in the local rest frame.

In order to study the energy-momentum tensor in more detail, we use a Gaussian profile in the laboratory frame to mimic the time dependence of the source, $\varphi(t, x) = \epsilon u(x) \exp[-(t - \nu)^2/\sigma^2]$: when $t - \nu$ is larger than a few σ , a time which can be identified with the injection time δt , the scalar source can be considered to vanish for all practical purposes. We consider the simple case where the spatial profile $u(x)$ has the form of a Gaussian with a homogeneous background, $u(x) = 1 + \exp(-\mu^2 x^2)$. (More general combinations of Gaussians and background are studied in [33].) Our results for the energy density in the local rest frame and for the local velocity are shown in Fig. 2. In order to gain some insight into these results, we next compare them with the evolution of the energy-momentum tensor in a free-streaming model as well as in hydrodynamics.

Our free streaming model is obtained by assuming that the distribution is massless noninteracting dust, composed of particles moving at the speed of light. In terms of the phase space distribution $f(t, \vec{x}, \vec{k})$, the components of the stress-energy tensor are given by

$$T^{\alpha\beta}(t, \vec{x}) = \int d^2k \frac{k^\alpha k^\beta}{k^0} f(t, \vec{x}, \vec{k}). \quad (4)$$

If we assume the phase space distribution at $t = 0$ to have the factorized form $f(\vec{x}, \vec{k}) = n(\vec{x})F(\vec{k}) = n(x)F(k)$, then at a later time

$$f(t, \vec{x}, \vec{k}) = n(\vec{x} - \vec{v}t)F(\vec{k}) = n(x - v_x t)F(k), \quad (5)$$

where $\vec{v} = \vec{k}/k^0$ is the particle velocity, and $F(k)$ only appears in (4) in an overall normalization factor. We choose $n(x)$ such that just after the energy injection has ended, the energy density in the laboratory frame coincides with the energy density we computed using AdS/CFT, and

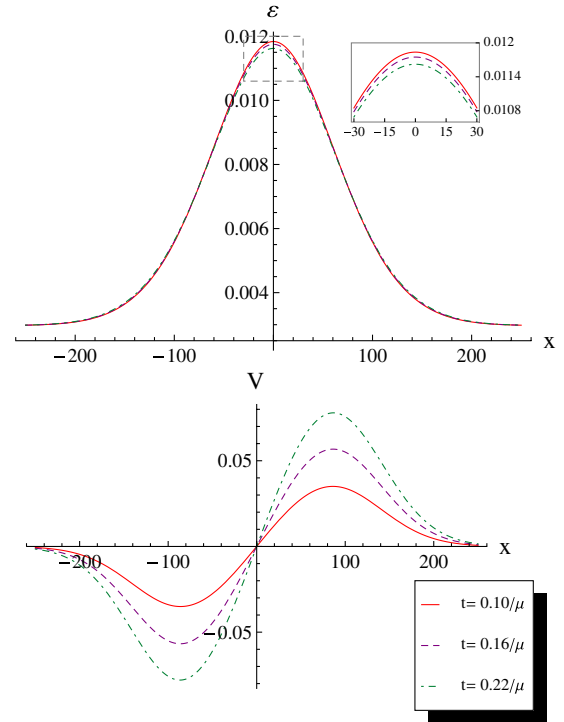


FIG. 2 (color online). The energy density in the local rest frame $\varepsilon = p_x + p_y$ (rescaled by $16\pi G_N$) and the plasma local velocity V for the solution with $\nu = 0.5$, $\sigma^2 = 0.1$, $\mu = 0.01$, and $\epsilon = 0.005$. As time increases, ε decreases in the region around $x = 0$ and increase for large $|x|$, while the velocity curves depart from the x axis.

we compare the pressure anisotropies in the local rest frame in Fig. 3.

Given the local velocity $V(t, x)$ and the energy density in the local rest frame $\varepsilon(t, x)$, we can ask what the stress-tensor would be if (first or second order) hydrodynamics

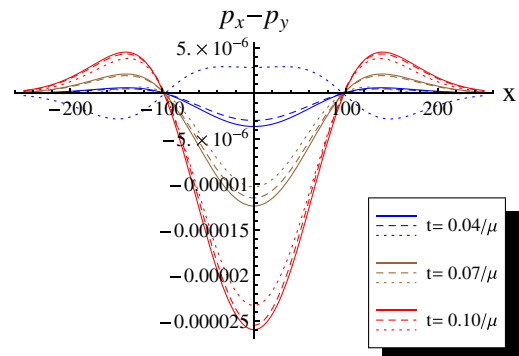


FIG. 3 (color online). Comparison of the pressure anisotropies (rescaled by $16\pi G_N$): AdS/CFT result in solid line, free streaming curves in dashed, second order hydrodynamics in dotted lines. The times plotted are shorter than those in Fig. 2 to ensure that the corrections to p_x and p_y coming from higher orders in the derivative expansion are negligible compared to the pressure anisotropies.

were valid at a given time t . Agreement with the stress tensor we computed using AdS/CFT would be a necessary condition for the validity of a (first or second order) hydrodynamical description from time t onwards. First order hydrodynamics requires the equation of state and the shear and bulk viscosities, which were obtained in [1,34] for the three-dimensional CFT under consideration. The first-order hydrodynamical stress tensor reads

$$T_{\text{viscous}}^{\alpha\beta} = (\varepsilon + p_{\text{ideal}})u^\alpha u^\beta + p_{\text{ideal}}\eta^{\alpha\beta} + \Pi_{(1)}^{\alpha\beta}. \quad (6)$$

Here, $p_{\text{ideal}} = \varepsilon/2$ and u^α is the local three-velocity of the fluid [which we determine from $V(t, x)$]. The first order viscous contributions to the energy-momentum tensor in flat three-dimensional space are given by [1]

$$\Pi_{(1)}^{\alpha\beta} \equiv -2\eta\sigma^{\alpha\beta} - \zeta\theta P^{\alpha\beta}, \quad (7)$$

where $P^{\alpha\beta} \equiv u^\alpha u^\beta + \eta^{\alpha\beta}$ is the projector onto space in the local fluid rest frame,

$$\sigma^{\alpha\beta} \equiv P^{\alpha\rho}P^{\beta\sigma}\left(\partial_{(\rho}u_{\sigma)} - \frac{1}{2}P_{\rho\sigma}\theta\right) \quad (8)$$

is the fluid shear tensor, and $\theta \equiv \partial_\rho u^\rho$ is the expansion. The shear viscosity η and bulk viscosity ζ are [1,34]

$$\eta = \frac{1}{16\pi G_N}\left(\frac{4}{3}\pi T\right)^2, \quad \zeta = 0, \quad (9)$$

where we define a local ‘‘temperature’’ $T(t, x)$ by using the thermodynamic relation that would be valid in equilibrium in the local rest frame,

$$\varepsilon = \frac{2}{16\pi G_N}\left(\frac{4}{3}\pi T\right)^3. \quad (10)$$

Using these ingredients, we have computed in [33] the pressure anisotropy in first order hydrodynamics. While qualitatively in agreement with our AdS/CFT results, it is too large to be in good quantitative agreement, so we conclude that first order hydrodynamics is not applicable in the early time window we can study [33].

Second order hydrodynamics for relativistic conformal fluids was derived in [2,3], providing a nonlinear generalization of Müller-Israel-Stewart theory. The second order contribution to the dissipative part of the stress tensor is

$$\Pi_{(2)}^{\alpha\beta} = \eta\tau_\Pi\left[\langle D\sigma^{\alpha\beta} \rangle + \frac{1}{2}\sigma^{\alpha\beta}\theta\right] + \dots, \quad (11)$$

where $\langle \rangle$ denotes the transverse traceless part [2], and $+\dots$ refers to terms that are not relevant here, as they either contain the Riemann or the Ricci tensor or terms that vanish for irrotational flow. In (11) D is the directional derivative along the 3-velocity, $D \equiv u^\mu \partial_\mu = -u_t \partial_t + u_x \partial_x$, and the new parameter τ_Π is the relaxation time for shear stress. For a strongly coupled conformal fluid it depends on harmonic numbers [35], in $2+1$ dimensions

$$\tau_\Pi = \frac{3}{4\pi T}\left[1 + \frac{1}{3}\text{harmonic}\left(-\frac{1}{3}\right)\right]. \quad (12)$$

A short calculation yields the hydrodynamic pressure anisotropy

$$p_x^{(H)} - p_y^{(H)} = 2\eta\left[-\theta + \tau_\Pi\left(D\theta + \frac{1}{2}\theta^2\right)\right]. \quad (13)$$

The pressure anisotropies obtained from second order hydrodynamics are compared to those from AdS/CFT and from free-streaming in Fig. 3. Throughout the time period in which we can trust our holographic solution free-streaming provides an excellent description of our holographic results. At the end of this time period, there is also consistency with second order viscous hydrodynamics. We are not able to make predictions for later times and cannot exclude the possibility that the holographic solution might again deviate from that of local viscous hydrodynamics at some later time. However, our results are fully compatible with the assumption that initial free streaming behavior turns into local hydrodynamic one within times smaller than $1/T$.

The reader may wonder why free streaming can reproduce the behavior of a strongly coupled gauge theory for any length of time. We do not have a complete answer to this question, but it is tempting to speculate that the short-time behavior of the stress-energy tensor is dominated by the singular behavior of the two-point correlation function of components of the stress-energy tensor. In a conformal theory, the correlation functions have a power-law dependence on the invariant space-time distance and diverge on the light cone. This suggests that free streaming of massless ‘‘particles’’ may reproduce the short-time behavior of these correlation functions [36].

In summary, we have investigated the evolution of the local pressure anisotropy in a strongly coupled field theory beginning from a spatially inhomogeneous, far off-equilibrium initial state. The anisotropy can be well described at early times by a free-streaming model. Towards the end of the early time window we can study, the stress tensor is consistent with the second order hydrodynamic stress tensor computed from the local energy density and fluid velocity. Our results are complementary to those of [32], who investigated the approach to hydrodynamics for a spatially homogeneous, but longitudinally expanding fluid. Taken together, these two results suggest that free streaming followed by second order viscous hydrodynamics may provide a valid description of the space-time evolution of the stress energy tensor in strongly coupled conformal gauge theories over the entire history. This would justify the standard approach to early time evolution of partonic matter in relativistic heavy ion collisions. However, given the very short time window our methods allow us to describe, more work is required to confirm whether the early-time agreement with second order hydrodynamics that we find is accidental or really signals the onset of a hydrodynamic regime. Specifically, we cannot

exclude the possible onset of violent equilibration dynamics at later times, as found in [37] for central, homogeneous, boost-invariant collisions. It would also be interesting to investigate different classes of initial conditions which prepare the nonequilibrium state in qualitatively different ways (e.g., IR injection of energy). It is possible that some of these classes would lead to different conclusions regarding, e.g., the validity of free streaming at early times.

We thank M. Heller, K. Rajagopal, and especially S. Minwalla for discussions. This research is supported by the Belgian Federal Science Policy Office, by FWO-Vlaanderen, by the Foundation of Fundamental Research on Matter (FOM), by Finnish Academy of Science and Letters, by the U.S. Department of Energy, by the BMBF, and by the Academy of Finland. A. B. is a Postdoctoral Researcher FWO and F. G. is Aspirant FWO.

-
- [1] V.E. Hubeny, S. Minwalla, and M. Rangamani, [arXiv:1107.5780](#).
- [2] R. Baier, P. Romatschke, D.T. Son, A.O. Starinets, and M.A. Stephanov, *J. High Energy Phys.* **04** (2008) 100.
- [3] S. Bhattacharyya, V.E. Hubeny, S. Minwalla, and M. Rangamani, *J. High Energy Phys.* **02** (2008) 045.
- [4] A. Adare *et al.* (PHENIX Collaboration), *Phys. Rev. Lett.* **98**, 162301 (2007).
- [5] L. Adamczyk *et al.* (STAR Collaboration), *Phys. Rev. C* **88**, 014902 (2013).
- [6] K. Aamodt *et al.* (ALICE Collaboration), *Phys. Rev. Lett.* **107**, 032301 (2011).
- [7] G. Aad *et al.* (ATLAS Collaboration), *Phys. Rev. C* **86**, 014907 (2012).
- [8] S. Chatrchyan *et al.* (CMS Collaboration), *Eur. Phys. J. C* **72**, 2012 (2012).
- [9] B.I. Abelev *et al.* (STAR Collaboration), *Phys. Rev. C* **80**, 064912 (2009).
- [10] K. Aamodt *et al.* (ALICE Collaboration), *Phys. Lett. B* **708**, 249 (2012).
- [11] B. Abelev *et al.* (ALICE Collaboration), *Phys. Lett. B* **719**, 18 (2013).
- [12] U.W. Heinz and R. Snellings, *Annu. Rev. Nucl. Part. Sci.* **63**, 123 (2013).
- [13] A. Adare, M. Luzum, and H. Petersen, *Phys. Scr.* **87**, 048001 (2013).
- [14] B. Müller and A. Schäfer, *Phys. Rev. D* **85**, 114030 (2012).
- [15] B. Schenke, P. Tribedy, and R. Venugopalan, *Phys. Rev. C* **86**, 034908 (2012).
- [16] C. Gale, S. Jeon, B. Schenke, P. Tribedy, and R. Venugopalan, *Phys. Rev. Lett.* **110**, 012302 (2013).
- [17] A. Bzdak, B. Schenke, P. Tribedy, and R. Venugopalan, *Phys. Rev. C* **87**, 064906 (2013).
- [18] B. Alver and G. Roland, *Phys. Rev. C* **81**, 054905 (2010); **82**, 039903 (2010).
- [19] H. Petersen, G.-Y. Qin, S. A. Bass, and B. Müller, *Phys. Rev. C* **82**, 041901 (2010).
- [20] G.-Y. Qin, H. Petersen, S. A. Bass and B. Müller, *Phys. Rev. C* **82**, 064903 (2010).
- [21] M. Martinez and M. Strickland, *Nucl. Phys. A* **848**, 183 (2010).
- [22] R. Ryblewski and W. Florkowski, *Phys. Rev. C* **85**, 064901 (2012).
- [23] This begins as the formation of a far-from-equilibrium black brane state, which subsequently relaxes to a static black brane.
- [24] S. Bhattacharyya and S. Minwalla, *J. High Energy Phys.* **09** (2009) 034.
- [25] J. Abajo-Arrestia, J. Aparicio, and E. Lopez, *J. High Energy Phys.* **11** (2010) 149.
- [26] T. Albash and C.V. Johnson, *New J. Phys.* **13**, 045017 (2011).
- [27] V. Balasubramanian, A. Bernamonti, J. de Boer, N. Copland, B. Craps, E. Keski-Vakkuri, B. Müller, A. Schäfer, M. Shigemori, and W. Staessens, *Phys. Rev. Lett.* **106**, 191601 (2011).
- [28] V. Balasubramanian, A. Bernamonti, J. de Boer, N. Copland, B. Craps, E. Keski-Vakkuri, B. Müller, A. Schäfer, M. Shigemori, and W. Staessens, *Phys. Rev. D* **84**, 026010 (2011).
- [29] H. Liu and S. J. Suh, [arXiv:1305.7244](#).
- [30] P.M. Chesler and L. G. Yaffe, *Phys. Rev. D* **82**, 026006 (2010).
- [31] G. Beuf, M.P. Heller, R. A. Janik, and R. Peschanski, *J. High Energy Phys.* **10** (2009) 043.
- [32] M. P. Heller, R. A. Janik, and P. Witaszczyk, *Phys. Rev. Lett.* **108**, 201602 (2012).
- [33] V. Balasubramanian, A. Bernamonti, J. Boer, B. Craps, L. Franti, F. Galli, E. Keski-Vakkuri, B. Müller, and A. Schäfer, *J. High Energy Phys.* **10** (2013) 082.
- [34] S. Bhattacharyya, R. Loganayagam, I. Mandal, S. Minwalla, and A. Sharma, *J. High Energy Phys.* **12** (2008) 116.
- [35] V.E. Hubeny and M. Rangamani, *Adv. High Energy Phys.* **2010**, 297916 (2010).
- [36] P. Calabrese and J.L. Cardy, *J. Stat. Mech.* (2005) P04010.
- [37] W. van der Schee, P. Romatschke, and S. Pratt, [arXiv:1307.2539](#).